The use of single-molecule FRET for the characterization of Holliday junctions containing human telomeric DNA: A methodological approach for nanoscale distance, mobility, and stability measurements.

Abeer FR Alanazi [1] Shozeb Haider, [1,2] Gary N Parkinson[1]

1. UCL School of Pharmacy, University College London, London WC1N 1AX, United Kingdom.

2. UCL Centre for Advanced Research Computing, University College London, London WC1H 9RN.

Corresponding author:

Shozeb Haider (shozeb.haider@ucl.ac.uk).

Gary N Parkinson (gary.parkinson@ucl.ac.uk)

ABSTRACT

Single-molecule analysis has emerged as a powerful biophysical technique, allowing the investigation of molecular interactions at unprecedented spatial resolutions. In this paper, we outline a step-by-step procedure for the design of DNA sequences to form Holliday junction structures containing repetitive telomeric sequences and exploring conformational dynamics using Single-Molecule Förster Resonance Energy Transfer (smFRET). We describe in detail the setup and optimization of the single-molecule fluorescence microscope, along with data acquisition and analysis procedures. Furthermore, we address potential challenges and provide troubleshooting strategies to ensure successful data collection and interpretation. The presented methodology serves as a valuable resource for researchers aiming to employ smFRET to study Holliday junctions and other biomolecular systems at the nanoscale, paving the way for further advancements in the field of single-molecule biophysics.

Key words: *Nanoimaging, DNA, chromophores, single molecules.*

INTRODUCTION

In recent years, the introduction of integrated benchtop single-molecule Förster Resonance Energy Transfer (smFRET) super-resolution microscopy hardware combined with intuitive software has revolutionized its applications to non-specialist users across a range of biophysical fields [1–3]. It provides new opportunities to investigate a range of biomolecules with exceptional sensitivity and precision, including the tracking dynamic molecular interactions in a variety of settings in 3D and in the real-time [4,5]. An understanding of the intricate and dynamic nature of DNA structures in various fundamental biological processes, such as genetic recombination, DNA repair, and replication is pivotal in transforming static structures to functional models. Holliday junctions (HJs) stand out as one such structure as they are key intermediates in homologous recombination, crucial for maintaining genomic integrity and facilitating genetic diversity [6]. Understanding the conformational dynamics and spatial organization of Holliday junctions at the single-molecule level is essential to unravel their functional significance and mechanistic intricacies [7]. Traditional ensemble-based techniques have provided valuable insights into the properties of Holliday junctions; however, they often average out the heterogeneity of these structures and lack the spatial resolution necessary to resolve individual conformational states. The smFRET leverages Förster Resonance Energy Transfer to precisely measure nanoscale distances between two fluorophores strategically positioned on the molecule of the interest offering data on the distances which vary from 30 to 120 Å [5]. Fluorophore pairs can be inserted during DNA solid phase synthesis to address interaction distances. By carefully designing the experiment and calibrating the setup, precise distance measurements can be obtained for individual Holliday junctions, enabling a deeper understanding of their structural properties, dynamics and revealing transient conformations that might be obscured in ensemble measurements.

In vitro Holliday junctions are artificially generated by combining oligonucleotides with complementary sequences located within the four branches. The annealing and hybridization process yields three potential conformations: an open state and two stacked orientations (Iso-I and Iso-II) [8]. These conformations are influenced by the type and presence of divalent metal ions in the solution. In the absence of cations, the negatively charged phosphates on the DNA strands remain unshielded, resulting in electrostatic repulsion. This repulsion causes the four arms of the junction to extend towards the corners of a square, forming an unstacked, fully extended conformation known as a square planar open-X structure. Conversely, the presence of divalent metal ions diminishes electrostatic repulsion, enabling the coaxial pairwise stacking of the helical arms to create a close-packed X-shaped structure with two-fold symmetry. This X-shaped stacked conformation encompasses two crossover isomers, Iso-I and Iso-II, distinguished by the stacking arrangement of the duplex arms. Each isomer consists of two exchanging strands on the junction's interface and two continuous strands on the outer edge, with the relative stability influenced by the local DNA sequence [9].

In human telomeric DNA sequences, the exchanging strands are either the C or G-rich strands. The telomeric G-rich strand, containing hexanucleotide repeats (5’-TAGGGT-3’), serves as the leading strand with measurements extending up to a few kilobases (kb). In contrast, the complementary C-rich strand is the lagging strand with the repeat sequence 5’-ACCCTA-3’ [10]. Initially believed to adopt a parallel configuration [11], Holliday junctions were later found to exhibit a right-handed antiparallel configuration through biochemical and structural studies [12]. In this configuration, two non-exchanging strands of opposite polarity define the external face of the Holliday junction, while two exchanging strands run in opposite directions, passing from one helical axis to another without physically crossing each other (Figure 1).

The dynamic nature of Holliday junctions allows them to assume multiple conformations. This work outlines a systematic methodology for applying single-molecule Förster Resonance Energy Transfer (smFRET) to study Holliday junctions formed from telomeric sequence using the Oxford Nanoimager. The investigations involve immobilized Holliday junctions folded as cruciform motifs containing human telomeric repeat sequences (Table 1). The study monitors changes in Holliday junction conformations induced by varying Mg^{2+}concentrations (Table 2) and demonstrates the Mg^{2+} dependence of Holliday junction stability in both stacked X-conformations over time. The paper aims to offer a detailed protocol for researchers, covering sample preparation, fluorophore labelling, immobilization, and data acquisition and analysis. It also addresses potential challenges, providing strategies to optimize experimental conditions and enhance data reliability from single-molecule measurements. By sharing these methods, the study aims to empower the scientific community to explore and understand the intricacies of Holliday junction topology, mobility, and stability at the nanoscale, contributing to a deeper comprehension of essential DNA processing mechanisms and their implications in health and disease. Moreover, these methods may aid in identifying selective ligands targeting telomeric Holliday junctions for potential therapeutic applications. The subsequent sections present the experimental procedures and analytical techniques that enable the probing of spatial organization and dynamic transitions of telomeric Holliday junctions at an unprecedented level of detail in the realm of single-molecule biophysics.

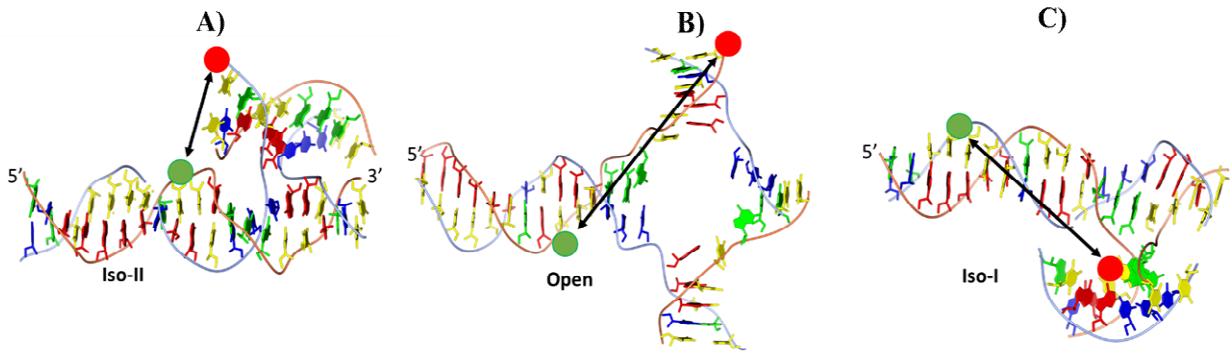

Figure 1: Holliday Junctions folded from our 2A-2B sequences showing transformation between the two isoforms through an open conformation. Backbone coloured in red is the G-rich strand and blue is the C-rich strand. Cy3 (green circle) attached, Cy5 is colour coded as red circle. Imaging CCP4 [13], Molecular Graphics and modelling building COOT [14].

METHODOLOGY

The smFRET experiments described herein are designed to place an immobile Holliday junction on a surface that allows for the Holliday junction to adopt various conformational states on a ms time scale [7].The obtained FRET efficiency values will be converted into donor-acceptor distances, with the highest FRET efficiency indicating the smallest distance between the donor and acceptor. Furthermore, the dynamic process of branch migration in Holliday junctions can be characterized by tracking FRET efficiency changes over time for individual junctions. The appropriate positioning of acceptor and donor labels on the DNA strands should allow us to follow conformational changes related to branch migration and/or the conformational transitions between Iso-I, open and Iso-II forms (Figure 1) [15].

Design of the DNA nucleotide sequences

The DNA sequences employed in this study were procured and synthesized from Eurofins Genomics with a synthesis scale of 0.2uM. Subsequently, they underwent purification via

High-Performance Liquid Chromatography (HPLC). Each oligonucleotide was labelled with either Cyanine fluorophores, Cy3 or Cy5. Holliday junctions are formed from 4 sequences 2A, 2B, 2C, 2D (Figure 2) (Table 1). These sequences are designed to efficiently fold as cruciform Holliday junctions via hybridization through stable stem loops capped by GTTC sequences.

DNA Holliday junction mobility

Holliday junctions play a pivotal role as intermediates in various genetic recombination processes and double-strand break repair. Typically characterized by a symmetrical sequence, these junctions exhibit mobility, allowing the four individual arms to navigate through the junction in a specific pathway that predominantly preserves base pairing. This mobility contributes to the dynamic nature of Holliday junctions, facilitating their involvement in essential genetic processes. If we design our experiments such that Holliday junctions mobility occurs on the ms time scale, then within the parameters of the data collection we will be able to observe these events as a single peaks allowing the application of the FRET distance relationship for our analysis. If the mobility occurs on shorter time scales, we will just see an average FRET efficiency. Within telomeric sequences the ACC repeat is expected to be point of residence during strand exchange in these mobile junctions in line with the crystallographic and biophysical data. We might then expect that this ACC residence will result in a consistent FRET signal.

Control sequences and sequence design

Sequence 2A is designed with biotin at the 3' end, facilitating attachment to Neutravidin for immobilization onto the support matrix. It is linked to a short run of deoxythymidines that concludes with a 7-nt CGTTTT(Cy3)T sequence containing a cyanine-3 fluorescent dye, as

illustrated in Figure 2. This sequence serves as a common linker and hybridizes to the cruciform-forming sequences 2B, 2C, and 2D, each containing a cyanine-5 fluorescent dye. Sequence 2B includes the telomeric sequence 5'-TAGGGT-3' and has a limited number of nucleotides in the loop of the complementary strands. Additionally, it features the ACC triplets. Holliday junctions are formed from the hybridization of 2A with 2C sequences. The black line represents the 2A sequence, and the orange line represents the 2C sequence. Notably, the 2C sequence has a longer sequence than 2B, enhancing stability, and contains the AGC triplets. Holliday junctions are also formed from the pairing of 2A with 2D sequences. The black line represents the 2A sequence, and the pink line represents the 2D sequence, which contains the ACC triplets. These Holliday junctions have the capability to fold into two potential anti-parallel conformations, Iso-I and Iso-II, resulting in distinct FRET signals due to the relative positions of the fluorophores.

Measuring Distances Between DNA Strands via smFRET in Holliday Junctions - the Experimental Procedure

(a) The sequence of interest was designed and synthesized, ensuring the Holliday junction contained specific DNA modifications relevant to the study. This facilitated the creation of cruciform Holliday junctions. DNA strands were labelled with cyanine fluorophores strategically to enable smFRET measurements. Immobilization for attachment was achieved by attaching labelled Holliday junction DNA to a suitable surface, like a functionalized coverslip or microfluidic chamber, at a low surface density. This allowed for single-molecule observations using biotin.

(b) Microscope Configuration: A single-molecule fluorescence microscopy system was set up with the following components

- High numerical aperture objective lens
- Excitation lasers for donor and acceptor fluorophores
- Appropriate filters and dichroic mirrors to separate donor and acceptor emissions
- Sensitive CCD camera for image acquisition

(c) Data Acquisition and Analysis

1. Data Collection: The sample was illuminated with an excitation laser corresponding to the donor fluorophore. Fluorescence emission data were collected from individual molecules, capturing time resolved fluorescence signals to record FRET events.

2. FRET Efficiency Calculation: FRET efficiency (E) for each molecule was calculated using the formula: E = I_A / (I_A + I_D), where I_A is the acceptor fluorescence intensity, and I_D is the donor fluorescence intensity [16].

3. Distance Determination: FRET efficiency (E) values were converted into distances using a calibration curve generated with identified donor-acceptor distances.

4. Data Analysis: The distribution of distances was analysed to uncover the conformational dynamics and interactions of the DNA strands in the Holliday junction.

Utilizing smFRET in this approach unveiled accurate distances between labeled DNA strands within Holliday junctions, offering a glimpse into the nuanced dynamics and fleeting

conformations of crucial DNA structures. Single-molecule techniques have exerted a substantial influence on optics, electronics, biology, and chemistry. In the realm of biological sciences, the examination of proteins and other intricate biological machinery was once constrained to ensemble experiments, rendering direct observation of their kinetics nearly unattainable.

MATERIALS AND METHODS

DNA Sequence Preparation

1. All DNA sequences utilized in this investigation were procured and synthesized from Eurofins Genomics, employing a synthesis scale of 0.2 μM.

2. The specific sequences are detailed in Table 1. These sequences were designed to facilitate branch migration and were subjected to purification via High-Performance Liquid Chromatography (HPLC).

3. Each oligonucleotide was labelled with Cyanine fluorophore Cy3 (FRET donor) and Cy5 (FRET acceptor) and Biotin (for surface immobilization). The anticipated Holliday junction confirmations were designed by combining sequences 2A with 2B, 2C, and 2D, as illustrated in Figure 1.

Table 1: The DNA sequences utilized in this study were synthesized by Eurofins Genomics and underwent HPLC purification. Biotin, Cy3, and Cy5 tags were incorporated at designated positions within the sequences for identification.

Sequence Name	Oligonucleotide sequence	Number of bases
2A	3' **Biotin**-TTTTCGTTTT(CY3) T5'	12
2B	5’GCAAAAAGGTTAGGGTTACTTGTAACCCTTGGGTTACTT(CY5) GTAACCCTAAC3'	50
2C	5'GCAAAAAGTTAGGCTTACTTGTAAGCCTCTTGAGGCTTACTT(CY5)GTAAGCCTAAC3'	54
2D	5'GCAAAAAGGTTAGGGGTTACTTGTAACCCTCTTGAGGGTTACT T(CY5)GTAACCCTAAC3’	54

DNA Sequences Utilized

The DNA sequences employed in this study were synthesized by Eurofins Genomics and subjected to purification via High-Performance Liquid Chromatography (HPLC). Noteworthy features of these sequences include the incorporation of Biotin, Cy3 (green), and Cy5 (red) tags at specific positions. Additionally, the C-rich and G-rich regions are indicated by red and blue font, respectively, while the ACC trinucleotide motif is underlined. Refer to Figure 1 for a visual representation of these features.

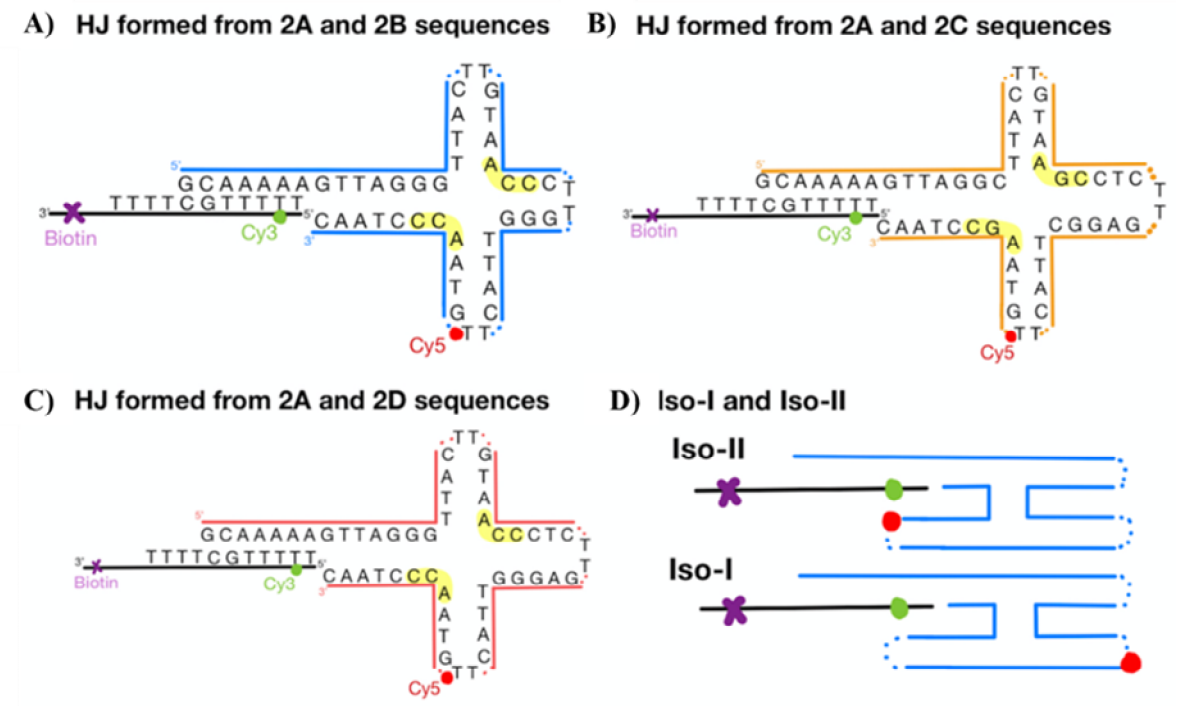

Figure 2: Holliday Junctions are depicted, constructed from our 2A, 2B, 2C, 2D sequences, and utilized in smFRET experiments. The 2A sequence is represented by a black line, featuring biotin (purple cross) and Cy3 (green circle) attachments, while Cy5 is color-coded as a red circle. The nucleotides highlighted in yellow indicate the location of the Holliday junction.

4. DNA Annealing Procedure

DNA annealing involves the heteroduplex formation of two complementary molecules (strand 2A) with regions of single-stranded DNA (ssDNA) (strands 2B, C, D). While this process can occur spontaneously, in vivo, specific classes of annealing proteins enhance its efficiency. In our experiments, the central portion comprising the top (2A) and bottom strands (2B, C, D) of either the Holliday junction or the dsDNA control was gradually brought together by annealing at a temperature range of (95 - 4°C). This was carried out to achieve a final concentration of 10 µM in 1× TAE with 12 mM $MgCl_2$, and additional details can be found in Table 1.

Subsequently, the annealed cruciform structure was hybridized to strand 2A at a temperature range of 50–4°C, maintaining a 1:1:1 molar ratio in 1× ligase buffer (New England BioLabs) [17]. This facilitated the hybridization of the sticky ends of the handles with their complementary overhangs on the central portion (2B, C, D).

5. Dilution of DNA annealed to appropriate concentrations

It is important to dilute DNA to appropriate concentrations and buffers from the initial storage stock solutions. Solutions require the following: use of double distilled H_2O, a TE solution containing Tris and EDTA following the protocol from Cheng et al. [18], where the TE buffer solution ensures the stability of the nucleic acids for long term storage while in solution.

Preparation of Stock Solutions – Long term Storage

1. Enzyme Stock Solution

A 5 ml enzyme stock solution was meticulously prepared for long-term storage. Initially, 1 g of Glucose Oxidase from Sigma-Aldrich was dissolved in 1 ml of distilled water, resulting in a final concentration of 1000 mg/mL. Subsequently, 100 mg of Catalase, also from Sigma-Aldrich, was diluted into 100 µL of distilled water to achieve the same concentration. To complete the stock solution, 100 µL of the Glucose Oxidase solution was combined with 4 µL of Catalase and 1 mL of 1M Tris-HCl at pH 8.0. The mixture was then adjusted to a total volume of 5 mL with distilled water, aliquoted into 50 µL portions in PCR tubes for convenient use, and stored at -20°C.

2. 1% w/v Glucose Solution Stock Solution

A 1% w/v Glucose solution stock solution was prepared by dissolving 0.5 g of glucose in 50 ml of distilled water. The resulting solution is stored in the fridge at 4°C.

3. Trolox Solution Stock Solution

For the Trolox solution stock solution, 0.1 g of Trolox was accurately weighed and dissolved in ethanol to make up a total volume of 100 mL, resulting in a 100 mM Trolox solution. Trolox, known for its ability to suppress blinking and enhance the prolonged emission of cyanine dyes, was employed to augment time resolution in accordance with studies [9,19].

4. 0.5M Magnesium Chloride Solution Stock Solution

A 0.5M Magnesium Chloride solution stock solution was prepared by dissolving 0.047 g of $MgCl_2$ in 1000 mL of distilled water.

5. 1M Sodium Chloride Solution Stock Solution

For the 1M Sodium Chloride solution stock solution, 0.058 g of NaCl was dissolved in 1000 mL of distilled water.

6. Biotinylated BSA Solution Stock Solution

To create a biotinylated BSA solution stock solution, 10 mg of BSA was dissolved in 10 mL of buffer solution, resulting in a final concentration of 1 mg/mL. This BSA-biotin solution was produced by dissolving 10 mg of BSA-biotin from Sigma-Aldrich in 10 ml of PBS and stored at -20°C in 500 µL aliquots.

7. Phosphate-Buffered Saline (PBS) Solution

For various experiments involving BSA-biotin and neutravidin solutions, a 1x PBS solution was prepared, consisting of 137 mM NaCl, 2.7 mM KCl, 8 mM Na_2HPO_4, and 2 mM KH_2PO_4.

8. TN Buffer Solution Stock Solution

The TN buffer solution stock solution was prepared by combining 10 μL of 1M Tris-HCl at pH 8.0, 10 μL of 5M NaCl, and 980 μL of distilled water.

9. Neutravidin Solution

A Neutravidin solution was created by dissolving 5 mg of unlabelled Neutravidin in 5 mL of PBS, also stored at -20°C in 500 μL aliquots [14].

Preparation of Imaging Buffer Solutions for FRET Experiment

Executing a FRET experiment demands precise imaging buffers, both with and without magnesium, prepared freshly to ensure optimal conditions during imaging. Our example protocol is provided below

1. Stock Solution Defrost and Combination

a. Defrost stock solution aliquots on ice to maintain their integrity.

b. Combine the defrosted aliquots as per Table 2, creating two imaging buffer solutions.

2. Airtight Sealing of Sample Solutions

Ensure the airtight sealing of sample solutions to preserve their composition and prevent exposure to oxygen, maintaining experimental accuracy.

3. Introduction into Flow Chamber

Introduce the imaging buffer into a six-channel ibidi μ-Slide VI 0.4 flow chamber immediately before the experiment commences. This ensures freshness and minimizes potential changes in solution properties.

4. Secure Sealing and Storage

a. Securely seal the chamber of the six-channel ibidi μ-Slide VI 0.4 in preparation for the FRET experiment.

b. Store the sealed chamber on ice to maintain the stability of the imaging buffer until it is ready for measurement.

5. Utilization of Nano Imager

Employ the Nano Imager, specifically the ONI system, for conducting the FRET experiment. The super-resolution microscopy capabilities of this system enhance the precision and quality of the experiment.

Lastly, this protocol not only ensures the freshness and stability of imaging buffers but also promotes efficiency in the execution of FRET experiments. The airtight sealing and immediate introduction into the flow chamber minimize potential changes in buffer properties, contributing to the reliability of the experimental results.

Surface Immobilization of DNA on μ-Slide VI 0.4 Flow Chambers

This refined protocol ensures meticulous handling of DNA samples, precise immobilization, and effective washing steps to create a stable and controlled environment for experiments involving DNA sequences. The strategic use of Neutravidin, Biotinylated BSA, and TN buffer contributes to the reliability and reproducibility of surface immobilization on μ-Slide VI 0.4 flow chambers as follows

1. Selection of Ideal Microscope Slides: Utilize microscope slides with multiple channels, exemplified by the µ-Slide VI 0.4 flow chamber (Figure 4). These slides are optimal for accommodating up to 6 independent DNA sequences within individual wells.

2. Careful Handling of DNA Samples: Handle DNA samples with care to minimize the risk of pH changes attributed to gluconic acid production, a by-product of the reaction [20].

3. Precise Pipetting for DNA Immobilization: Exercise precision while pipetting DNA-containing solutions to facilitate the immobilization of folded DNA Holliday junctions onto the slides (Figure 3).

4. Immobilization via Neutravidin: Immobilize biotinylated DNA sequences onto the slides using Neutravidin (ThermoFisher). Neutravidin's strong affinity for biotin ensures stable and specific binding, crucial for reliable immobilization.

5. Pre-Wash with Biotinylated BSA: Prior to DNA addition, pre-wash the slides with Biotinylated Bovine Serum Albumin (BSA). BSA, known to adsorb to glass, facilitates the binding of biotinylated molecules through multivalent avidin proteins, such as Neutravidin [19].

6. Washing Steps with TN Buffer: Implement washing steps between each stage using TN buffer, following the formulation by [21]. TN buffer comprises 10 µl of 1M Tris-HCl at pH 8.0, 10 µl of 5M NaCl, and 980 µl of distilled water. This buffer maintains a stable pH environment and provides optimal conditions for DNA immobilization.

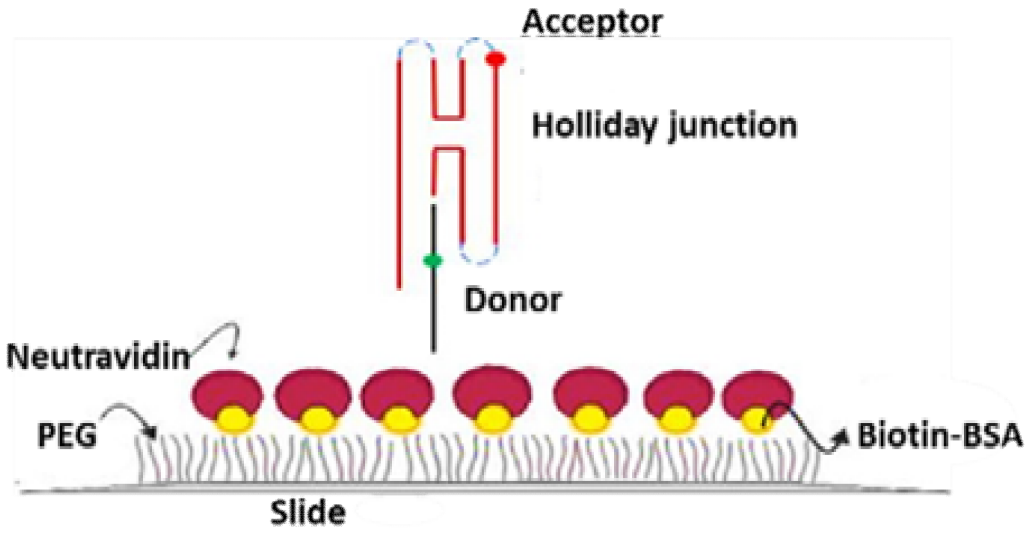

Figure 3: Shows the Surface immobilization strategies for smFRET experiments.

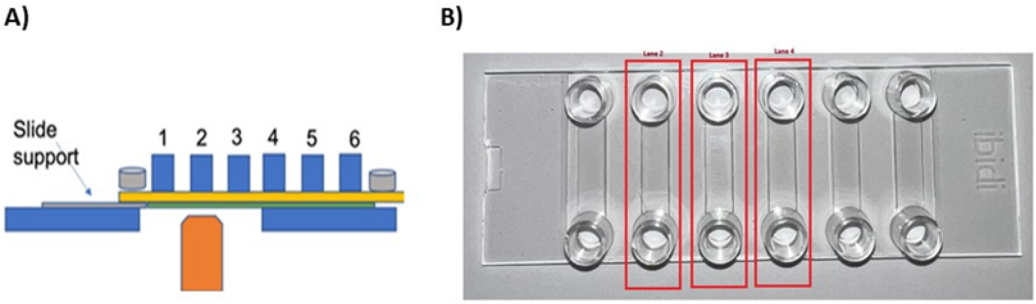

Figure 4: (a) The Ibid µ-Slide VI 0.5 is depicted, with labeled lanes for reference. The dimensions of the channel are specified as 17mm in height and 3.8mm in width, and the glass bottom has a thickness of no. 1.5H. (b) An illustration is presented to showcase the concept of using a coverslip and the 6-channel slides. Notably, lanes 1 and 6 are rendered impractical for use, while lanes 2 and 5 can be utilized with the support of a slide.

Experimental setup for the DNA sequences 2AB with zero and high magnesium concentration

1. PBS Wash

Before each FRET experiment, washed one well in a 6-well ibidi µ-Slide three times with 60 µl PBS to ensure a clean well surface for subsequent coating. Throughout the experiment, careful attention was given to avoid scratching the well's surface, and solutions were pipetted at the same position within the well.

2. BSA-Biotin Coating

Added 60 µl BSA-biotin to the well and incubated at room temperature for 5 minutes. This step promoted the adhesion of BSA-biotin molecules, forming a stable coating.

3. BSA-Biotin Removal and PBS Wash

Removed the BSA-biotin solution and washed the well three times with 60 µl PBS. Ensured gentle pipetting to avoid scratching the well surface, maintaining coating integrity.

4. Neutravidin/Streptavidin Binding

Added 60 µl neutravidin or streptavidin solution to the well and incubated at room temperature for 5 minutes. This facilitated the binding of neutravidin or streptavidin to BSA-biotin, creating a stable platform for subsequent interactions.

5. Neutravidin/Streptavidin Removal and PBS Wash

Removed the neutravidin/streptavidin solution and washed the well three times with 60 µl PBS. Ensured the removal of any unbound molecules, enhancing the purity of the coated surface.

6. DNA in TN Buffer Binding

Added 60 µl DNA in TN buffer to the well and incubated for 5 minutes at room temperature. Adjusted the DNA concentration as needed. This step enabled the binding of DNA to the avidin-coated surface.

7. TN Buffer Wash

Washed the well three times with TN buffer. The DNA was expected to be stably bound to avidin in TN buffer until the addition of the Imaging Buffer, immediately before each imaging session, the TN buffer was replaced with 50µl of imaging buffer or Mg^{2+} imaging buffer.

8. The imaging buffer featured an oxygen-scavenging system involving catalase and glucose oxidase [22]. with the same concentration of Na^{+} and with 50mM Mg^{2+} and without (See Table 2).

9. A coverslip was carefully placed over the top of the well, creating a sealed chamber free of air bubbles.

10. Once the wells were prepared, single-molecule FRET measurements were conducted using the Nano Imager called ONI (Oxford Nano Imaging, Oxford, UK).

This protocol, performed in our lab, optimized coating efficiency and minimized the risk of spillage associated with the nominal well capacity. The sequential steps ensured a stable and clean coating for subsequent experiments, contributing to the reliability of the obtained results.

Table 2: Imaging buffer with different concentrations of Mg^{2+}

Final concentration of Mg^{2+} (mM)	**0**	**50**
Enzyme stock (µl)	10	10
Glucose stock (µl)	80	80
Trolox stock (µl)	2	2
Magnesium Chloride (Stock 500 mM Mg^{2+}) (µl)	0	20
NaCl 1M (µl)	6.7	6.7
Distilled water (µl)	101.3	81.3
Total (µl)	200	200

Imaging using the Nanoimager, ONI (Oxford Nanoimaging, Oxford, UK)

1. The ONI Nano Imager S Mark II microscope was utilized to measure the single-molecule FRET (smFRET) efficiency of telomeric DNA sequences and observe FRET emission, as depicted in Figure 5.

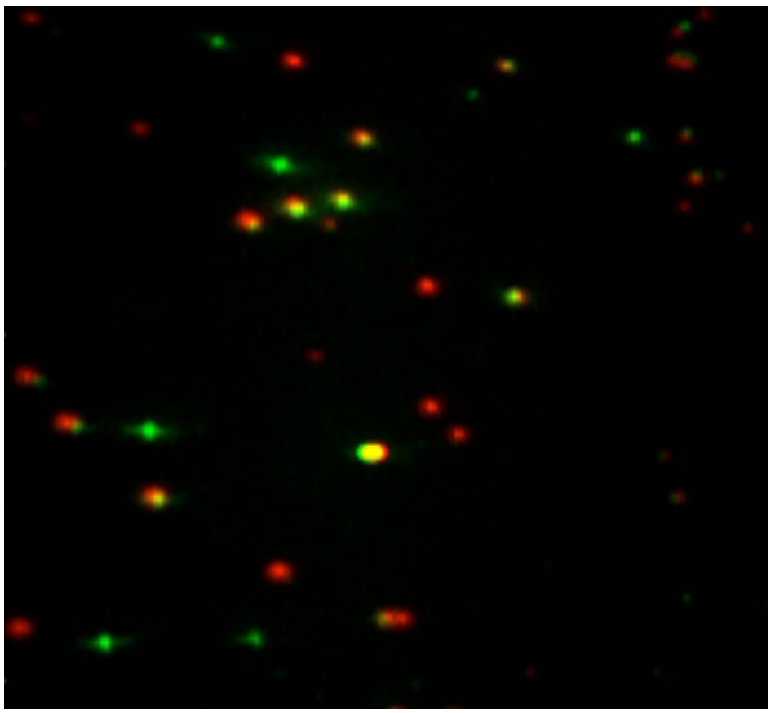

Figure 5: Sample frame showing multiple immobilized DNA Holliday junction molecules. Cy3 (green) and Cy5. (red) emission observed.

2. All smFRET data collection conducted using the Oxford Nanoimager (ONI) machine with settings: 10ms exposure time, 100Hz frequency, and 1000 image captures per 10s.

3. Employed a 532nm green laser and a 639nm red laser at 24% intensity of 1W power.

4. Observed immobilized DNA Holliday junction molecules through Cy3 (green) and Cy5 (red) emission with the 532nm green laser. NimOS ONI software (Version 1.18.3) facilitated data

acquisition and analysis, using the number of photons counts and localization, while disregarding background noise.

5. Prior to the experiment, calibrated the ONI device and NimOS software using imaging buffer to confirm X, Y, and Z coordinates for optimal focus and resolution.

6. Collected data included quantitative measurements of positions, energy transfer efficiency, and time taken.

7. Analyzed data to determine the distance between fluorophores Cy3 (donor) and Cy5 (acceptor) based on FRET efficiency, correlating with Holliday junction conformation (Figure 6abc).

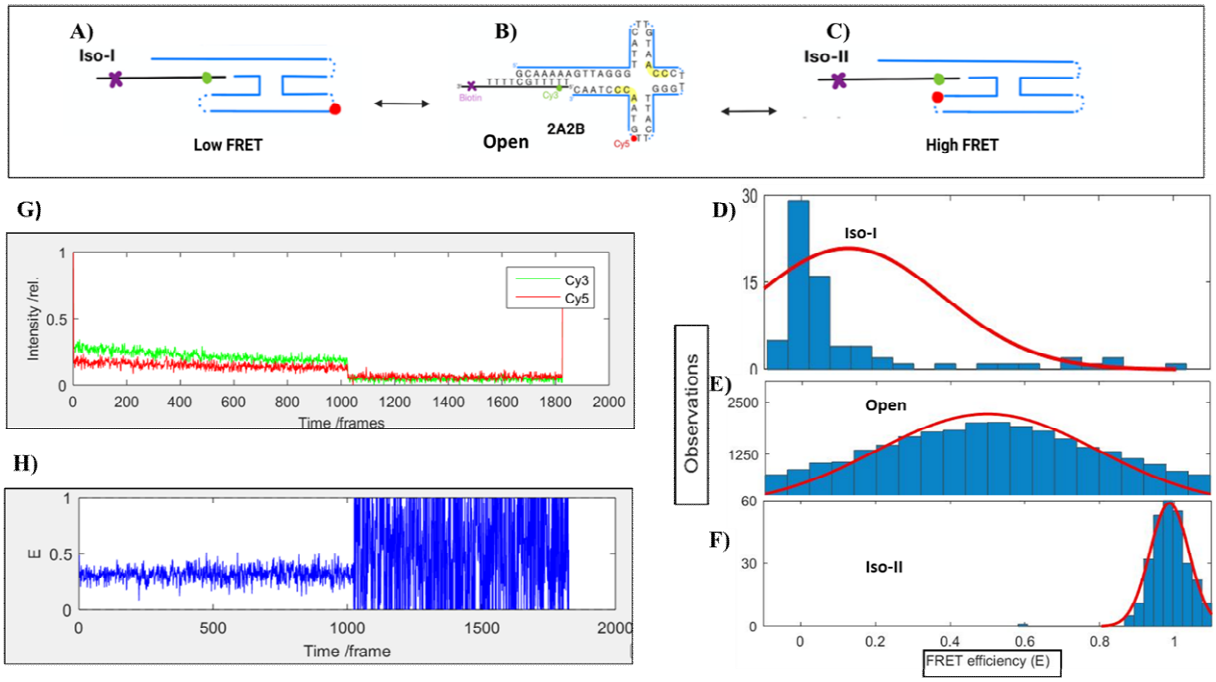

Figure 6: The smFRET analysis time-traces of short four arms in the Holliday junctions sequence 2A2B at 0 mM Mg^{2+} reveals distinct conformations: low FRET Iso-I (A), medium FRET (B), and high FRET Iso-II (C). The FRET histogram (D, E, F) displays single-molecule data that features transitions from the lowest to the highest FRET states, highlighting the changes between Iso-I and open, Iso-II. The two-colour smFRET data, utilizing a Donor (Red) and an Acceptor (Green), captures the dynamic energy transfer processes occurring between Iso-I and Iso-II conformations (G), where the associated

FRET efficiency (H) provides the crucial distance relationship metric for understanding both the conformational topology and residence time between states.

8. Quantitative data on the distance between Cy3 and Cy5 were determined using WinCoot software and PDB IDs for Holliday junctions in the three conformations.

9. To detect each transition of Holliday junctions, the optimum exposure time of the camera was chosen for each Mg^{2+}concentration. An exposure time of 50ms was used for 0 mM Mg^{2+} concentration.

10. Data acquisition and the selection of single-molecule FRET traces were executed using the ONI software NimOS (Version 1.18.3, ONI). The processing of Holliday junctions and the grouping particles into sets is a vital step in data analysis, here involving the categorization of particles based on specific criteria that involves several sequential steps. Initial data acquisition entails collecting precise and accurate experimental data, predominantly fluorescence signals, from the particle over time. Appropriate preprocessing of the raw data is necessary to eliminate noise and normalize for variations. The calculation of FRET efficiency can then be carried out based on changes in donor and acceptor fluorescence intensities over time. Classification of particles based on its FRET efficiency is useful to identify trends and correlations within the particles in order to understand particle's behaviour. The criteria for grouping can vary, such as FRET efficiency levels or spatial behaviours.

11. To generate our histogram Figure 6 (D,E,F), the initial step involves the collection of a dataset containing relevant values. Subsequently, the range of these values is divided into intervals, known as bins, as part of the binning process. The frequency of occurrences within each bin is then counted, forming the basis for constructing a bar chart. This chart visually represents each bin on the x-axis and its corresponding frequency on the y-axis, with the height of each bar indicating the frequency of data points in that bin. Optionally, normalization can be applied to represent frequencies as proportions or percentages formatted into a histogram,

showing variable and frequency. The resulting histogram serves as a visual summary, allowing for the quick and intuitive interpretation of the data's distribution, central tendencies, and variability.

12. In the stacked-X conformation (Iso-I and Iso-II), the four arms of the Holliday junction are tightly stacked on top of each other, forming a well-ordered cross structure. The histograms for Iso-I have peaks at 0.1 FRET efficiency, classified with low FRET. Shown in in Figure 1C and Figure 6 D, the red and green intensities signify distinct conformations. For Iso-II exhibit peaks at 0.8 FRET efficiency, indicative of a high FRET state. Figure 1A and Figure 6F illustrate the red and green intensities, providing insight into the distinct conformations associated with Iso-II.

13. The open square planar conformation involves a more dynamic and flexible arrangement of the four arms, with a separation between the arms of the junction in a flat, square planar structure. Analysing the histograms for the 'Open' conformation shows peaks at 0.5 FRET efficiency, corresponding to medium FRET levels. As depicted in Figure 1A and Figure 6 E, the interplay of red and green.

14. Through continuous monitoring of the donor (green) and acceptor (red) fluorescence signals, we acquire a comprehensive understanding of the intricate dynamics and energy transfer processes within the system. This thorough analysis of emitted signals enables a nuanced exploration of the intricate interplay between donor and acceptor molecules, revealing insights into the system's molecular-level behavior over time. In Figure 6 (G) the temporal significance is emphasized, with 1000 frames corresponding to 10 seconds. This temporal framework facilitates the determination of residence states for each conformation, providing valuable insights into the transitions from Iso-I to Iso-II.

15. Analysis of FRET efficiency (Figure 6. H) can be beneficial in probing changes in structures within the system, reflecting the effectiveness of energy transfer between the donor and acceptor, as determined from the collected intensity data. Analysing fluctuations in FRET efficiency offers valuable insights into the dynamic nature of energy transfer processes (state) within the smFRET system.

16. Monitoring the dynamic nature of a system is possible using real-time systems that offer instantaneous feedback. Through the continuous monitoring of the donor (green) and acceptor (red) fluorescence signals, we can acquire a comprehensive understanding of the intricate dynamics and energy transfer processes within the system. In Figure 6 (G) the temporal significance is emphasized, with 1000 frames corresponding to 10 seconds. This temporal framework facilitates the determination of residence states for each conformation, providing valuable insights into the transitions from Iso-I to Iso-II.

17. FRET efficiency, shown in Figure 6 H, can be used to probe changes in the system, reflecting the effectiveness of energy transfer between the donor and acceptor, as determined from the collected intensity data. Analysing fluctuations in FRET efficiency offers valuable insights into the dynamic nature of energy transfer processes (state) within the smFRET system.

The timescale of these changes fell below the limitations of ONI, manifesting as a distinct line connecting the two FRET efficiency populations. In this experimental scenario, the molecule appeared to lack low (<0.1) FRET efficiency states, or if present, these states were too brief to be detected. This observation is grounded in the cutoff below the FRET value of 0.1, considered as negligible background noise or bleed between the detection channels [23].

Additionally, In the experimental protocol, specific details were emphasized to ensure accurate and insightful measurements. For the Mg^{2+}concentration of 0.01mM, an exposure number of 500 was selected, and the temperature during measurements for sequence 2A2B was meticulously maintained at 29°C. Prior to each FRET measurement, a crucial step involved calibrating the microscope, ensuring the Nanoimager was poised for precise assessments. The Nanoimager systematically gauged the energy transfer between the two fluorophores, particularly focusing on the donor-to-acceptor transfer to discern the spatial distance between them. Employing the sophisticated technique of total internal reflection fluorescence (TIRF), single-molecule FRET (smFRET) experiments were performed on the DNA samples using the Nanoimager (Figure 7). This method, leveraging localized excitation and fluorescence observation near the surface, significantly enhanced the sensitivity and precision of the FRET measurements.

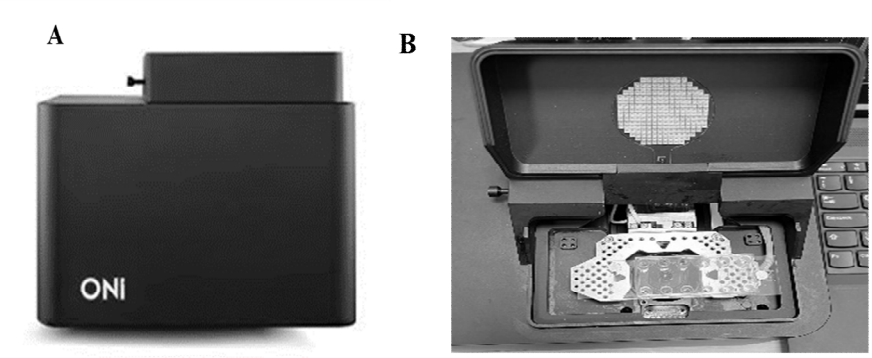

Figure 7: (**A**) Oxford NanoImager (ONI, University of Oxford). (**B**) Internal slide loading system for Oxford NanoImager. Camera aligned to slide lane with active experiment.

Probing the Nano Realm: Advantages of Single-Molecule Förster Resonance Energy Transfer (smFRET) Studies in Unravelling Molecular Dynamics

Single-Molecule Förster Resonance Energy Transfer (smFRET) studies offer several advantages, making them a powerful tool for investigating molecular interactions and conformational dynamics. Some key advantages include

1. High Spatial Resolution

smFRET provides information at the single-molecule level, allowing researchers to observe molecular interactions with unprecedented spatial resolution. This is particularly valuable for studying heterogeneous or dynamic systems.

2. Observation of Individual Molecules

The ability to study individual molecules eliminates the need for ensemble averaging, providing insights into the behavior of individual molecules within a population.

3. Dynamic Range

smFRET studies offer a wide dynamic range, enabling the detection of subtle conformational changes and interactions that might be averaged out in bulk experiments.

4. Real-Time Monitoring

smFRET allows real-time monitoring of dynamic processes, providing information on the kinetics of molecular interactions and conformational changes.

5. Detection of Heterogeneity

Heterogeneous populations within a sample can be identified, allowing the characterization of multiple states or conformations that may coexist.

6. Study of Rare Events

smFRET can capture rare events that might be obscured in ensemble measurements, providing a more comprehensive understanding of complex biological processes.

7. Single-Molecule Tracking

It enables the tracking of individual molecules over time, facilitating the observation of transient states and transitions.

8. Insights into Biomolecular Systems

Applied to biomolecular systems, smFRET can shed light on the dynamic behavior of biomolecules, including DNA, RNA, proteins, and their interactions.

9. Applications in Structural Biology

smFRET can be applied to study the structural dynamics of biomolecules, providing complementary information to traditional structural biology techniques.

10. Single-Molecule Fingerprinting

Each molecule acts as its own probe, allowing for "fingerprinting" of individual molecules and providing a more detailed understanding of their behavior.

In summary, smFRET studies offer a unique and detailed perspective on molecular interactions and dynamics, contributing to our understanding of complex biological processes.

Limitations of Single-Molecule Förster Resonance Energy Transfer (smFRET) Studies

While smFRET is a potent method for investigating molecular interactions and conformational dynamics, several considerations and limitations impact its application in this study

1. Sample Complexity

The success of smFRET experiments relies on the purity and homogeneity of the sample. Complex mixtures or impurities may introduce noise and artifacts.

2. Sample Preparation Challenges

Labelling DNA strands with fluorophores can potentially alter their native structure. Ensuring minimal perturbation during the labelling process is crucial.

3. Quantification Issues

Accurate quantification of FRET efficiency and distance measurements can be challenging due to factors such as photobleaching, fluorophore stoichiometry variations, and instrument calibration.

4. Low Signal-to-Noise Ratio

smFRET measurements, especially with single molecules, may suffer from a relatively low signal-to-noise ratio, making it challenging to detect weak or transient interactions.

5. Limited Temporal Resolution

The finite time required for data acquisition may restrict the ability to capture very rapid conformational changes or interactions.

6. Limited Spatial Resolution

While offering nanometre-scale precision, smFRET may not provide atomic-level structural details. Finer resolution may necessitate complementary techniques.

7. Surface Immobilization Effects

Immobilizing molecules on a surface can influence their behavior compared to their dynamic state in solution, potentially introducing artifacts.

8. Heterogeneity

Biomolecular systems often exhibit diverse behaviors, and smFRET may not capture the full spectrum of conformational states or interactions.

9. Limited Applicability

smFRET is most effective when two fluorophores can be strategically attached, limiting its applicability to all biomolecular complexes or systems.

10. Data Analysis Challenges

Analysing smFRET data is intricate, requiring specialized software. Interpretation involves assumptions and models, introducing uncertainties.

11. Cost and Technical Expertise

Establishing and maintaining a single-molecule fluorescence microscope with smFRET capabilities is costly and demands expertise in optics and data analysis.

Clearly researchers must carefully consider these limitations in experimental design and result interpretation. Despite these limitations, smFRET remains an invaluable tool for probing nanoscale molecular interactions, offering insights that complement other biophysical techniques with opportunities to further enhance it capabilities.

ACKNOWLEGEMENTS

AFRA would like to thank the Ministry of Education and King Abdullah scholarship program in Saudi Arabia for their financial and academic support. The authors would also like to thank Dr. Franky Djutanta at Oxford Nanoimaging for constructive discussions.

ETHICS DECLARATION

CONFLICT OF INTEREST

The authors declare no conflict of interest.

REFERENCES

1. Long X, Parks JW, Stone MD. Integrated magnetic tweezers and single-molecule FRET for investigating the mechanical properties of nucleic acid. Methods. 2016;105:16–25.

2. Li C, Li Y, Zhang Y, Zhang C. Single-molecule fluorescence resonance energy transfer and its biomedical applications. TrAC Trends in Analytical Chemistry. 2020;122:115753.

3. Qiao Y, Luo Y, Long N, Xing Y, Tu J. Single-Molecular Förster Resonance Energy Transfer Measurement on Structures and Interactions of Biomolecules. Micromachines. 2021;12:492.

4. Schärfen L, Schlierf M. Real-time monitoring of protein-induced DNA conformational changes using single-molecule FRET. Methods. 2019;169:11–20.

5. Quast RB, Margeat E. Single-molecule FRET on its way to structural biology in live cells. Nat Methods. 2021;18:344–5.

6. Song Q, Hu Y, Yin A, Wang H, Yin Q. DNA Holliday Junction: History, Regulation and Bioactivity. IJMS. 2022;23:9730.

7. McKinney SA, Déclais A-C, Lilley DMJ, Ha T. Structural dynamics of individual Holliday junctions. Nat Struct Biol. 2003;10:93–7.

8. Lilley DMJ. Structures of helical junctions in nucleic acids. Quart Rev Biophys. 2000;33:109–59.

9. Müller DJ, Sapra KT, Scheuring S, Kedrov A, Frederix PL, Fotiadis D, et al. Single-molecule studies of membrane proteins. Current Opinion in Structural Biology. 2006;16:489–95.

10. Haider S, Li P, Khiali S, Munnur D, Ramanathan A, Parkinson GN. Holliday Junctions Formed from Human Telomeric DNA. J Am Chem Soc. 2018;140:15366–74.

11. Sigal N, Alberts B. Genetic recombination: The nature of a crossed strand-exchange between two homologous DNA molecules. Journal of Molecular Biology. 1972;71:789–93.

12. Murchie AIH, Clegg RM, Krtzing EV, Duckett DR, Diekmann S, Lilley DMJ. Fluorescence energy transfer shows that the four-way DNA junction is a right-handed cross of antiparallel molecules. Nature. 1989;341:763–6.

13. Adams PD, Afonine PV, Bunkóczi G, Chen VB, Davis IW, Echols N, et al. PHENIX : a comprehensive Python-based system for macromolecular structure solution. Acta Crystallogr D Biol Crystallogr. 2010;66:213–21.

14. Emsley P, Lohkamp B, Scott WG, Cowtan K. Features and development of Coot. Acta Crystallogr D Biol Crystallogr. 2010;66:486–501.

15. Karymov M, Daniel D, Sankey OF, Lyubchenko YL. Holliday junction dynamics and branch migration: Single-molecule analysis. Proc Natl Acad Sci USA. 2005;102:8186–91.

16. Long X, Stone MD. Kinetic Partitioning Modulates Human Telomere DNA G-Quadruplex Structural Polymorphism. Rybenkov VV, editor. PLoS ONE. 2013;8:e83420.

17. Gibbs DR, Mahmoud R, Kaur A, Dhakal S. Direct unfolding of RuvA-HJ complex at the single-molecule level. Biophysical Journal. 2021;120:1894–902.

18. Cheng Y-J, Guo W-W, Yi H-L, Pang X-M, Deng X. An efficient protocol for genomic DNA extraction fromCitrus species. Plant Mol Biol Rep. 2003;21:177–8.

19. Michalet X, Weiss S, Jäger M. Single-Molecule Fluorescence Studies of Protein Folding and Conformational Dynamics. Chem Rev. 2006;106:1785–813.

20. Hyeon C, Lee J, Yoon J, Hohng S, Thirumalai D. Hidden complexity in the isomerization dynamics of Holliday junctions. Nature Chem. 2012;4:907–14.

21. Götz M, Wortmann P, Schmid S, Hugel T. Using Three-color Single-molecule FRET to Study the Correlation of Protein Interactions. JoVE. 2018;56896.

22. Roy R, Hohng S, Ha T. A practical guide to single-molecule FRET. Nat Methods. 2008;5:507–16.

23. Lee S, Lee J, Hohng S. Single-Molecule Three-Color FRET with Both Negligible Spectral Overlap and Long Observation Time. Mayer C, editor. PLoS ONE. 2010;5:e12270.

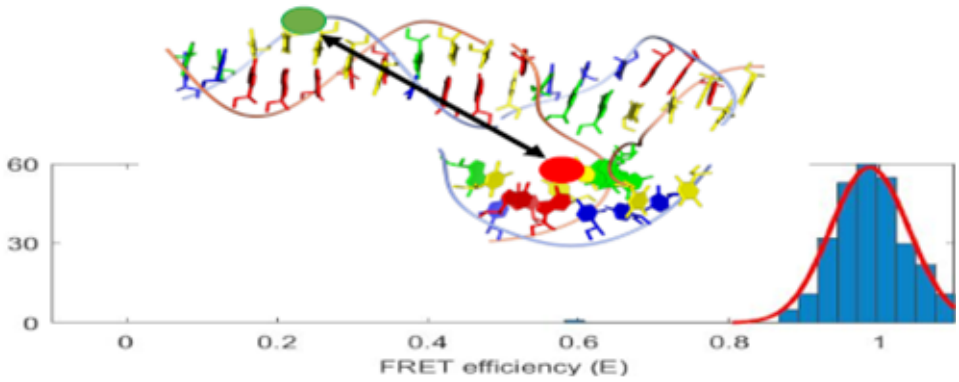
60
30
0
0
0.2
0.4
0.6
0.8
1
FRET efficiency (E)